Development of a High Gain, Dual-Band and Two-Layer Miniaturized Microstrip Antenna for 5.8 GHz ISM and 10 GHz X-Band Applications

İsa Ataş [1], Teymuraz Abbasov [2], and Muhammed B. Kurt [3]

[1] Vocational School of Technical Sciences
Dicle University, Diyarbakır, 21280, Turkey
isa_atas@dicle.edu.tr

[2] Department of Electrical and Electronics Engineering
İnönü University, Malatya, 44280, Turkey
teymuraz.abbasov@inonu.edu.tr

[3] Department of Electrical and Electronics Engineering
Dicle University, Diyarbakır, 21280, Turkey
bkurt@dicle.edu.tr

Abstract ─ In this study, it is explained how to increase the gain of a two-layer stacked miniaturized microstrip patch antenna (MPA) operating at 5.8 GHz and 10 GHz step by step by combining several different methods used in the literature for performance improvement of MPAs. A commonly used FR4 substrate material was preferred to design and produce the antenna. For electromagnetic modeling of the prototype structure, numerical analysis, and optimization, ANSYS HFSS was used. The performance of the proposed antenna was evaluated in terms of return loss (RL), surface current distribution, radiation patterns and gain/directivity. To confirm the study, the simulation results were compared with the measurements taken over the antenna prototype and good agreement has been achieved. The peak gain values of the proposed antenna at 5.8 GHz and 10 GHz are obtained as 4.11 dBi and 7.15 dBi, respectively.

Index Terms ─ Dual-band, gain, impedance matching, microstrip antenna.

I. INTRODUCTION

Due to the rapid increase in communication technologies and the demand for different frequency applications in wireless devices, compact structured and multi-band MPAs offer the best solution. These antennas can be integrated with various portable devices for efficient data transmission and reception [1].

MPA has many advantages, but it has two main disadvantages as low gain and narrow bandwidth. Various methods are used to overcome these disadvantages. These methods are:

a. Etched slots on the patch [2],
b. Appropriate feeding [3],
c. Defected Ground Structure (DGS) [4],
d. Adding different shaped parasitic patches to the patch at appropriate positions [5],
e. Multi-layer structure [6].

Although these methods were used to increase the gain and bandwidth of the antenna in the literature, in our study we focused on increasing the number of working band and the gain of an antenna by using these methods. As far as we can see in the literature, DGS method was used to increase the bandwidth of an antenna. In our study, we used it to increase the gain of our antenna.

There have been numerous designs of double-band MPAs over the past decades, especially for wireless communications, 3.5 GHz WiMAX (3.3-3.7 GHz), 5.5 GHz (5.150-5.825 GHz) and/or 2.4 GHz (2.4-2.483 GHz) WLAN and 10 GHz (8-12 GHz) radar applications. Some of those were planar multiple shaped strips with binomial curved conductor support [7], meander line and a patch in the form of a reverse toothbrush [8], microstrip line feeder split ring metamaterial structure [9], DGS with multi-strip monopole antenna [10], inverted-F antenna (IFA) structure [11], H-shaped antenna for GPS and Wi-Fi applications [12], microstrip antenna with improvement in performance using DGS [13], extended L-shaped multiband antenna for wireless applications [14], multi-layer stacked patch antenna [15]. However, most of these antennas are large in size. As far as literature studies are concerned, most of the techniques used for compact size and multi-band antennas are complicated due to the necessity of additional structures or due to their large size. In order to design a small and compact wireless device, it is necessary to miniaturize the antenna size accordingly.

The ITU (International Telecommunication Union)

Submitted On: December 25, 2018
Accepted On: March 27, 2019

had originally reserved a portion of the RF spectrum globally for industrial, scientific and medical (ISM) applications [16]. One of the ISM bands, which has center frequency of 5.8 GHz is between 5.725 GHz and 5.875 GHz. The frequency band of 5.8 GHz is especially important for high speed Wi-Fi routers, FPV (First Person View) applications where antennas with smaller dimensions and profile are desirable. This allows users to access the microwave spectrum without the need for regulations and restrictions that can be applied elsewhere [17, 18].

In radar engineering, X-band (8.0 to 12.0 GHz) is used extensively for detection and identification of reflective objects such as aircraft, ship, space vehicle, vehicle, human and natural environment [19].

The higher the frequency, the smaller the antenna dimensions. Since the our antenna was designed initially according to 10 GHz and then a second operating frequency was added at a frequency of 5.8 GHz, the designed antenna dimensions were smaller than the antenna designed at the 5.8 GHz band. Thus, an antenna operating in the 5.8 GHz band was designed with the small dimensions of 10 GHz. In addition, in the literature search as far as we have seen, we did not find any antenna that works in both 10 GHz and 5.8 GHz as dual band.

This study proposes a new design approach for gain improvement of two-layer stacked MPA with dual band operating at 5.8 GHz ISM and 10 GHz X-Band Radar applications.

This article is organized as follows. Section II covers the antenna configuration and design procedure. Simulation and measurement results are discussed in Section III and comparison tables are given in this section. Section IV contains the result of this study.

II. DESIGN SPECIFICATIONS OF PROPOSED ANTENNA

This section presents a description of the geometric configuration and basic steps involved in the design of the proposed antenna.

A. Antenna configuration

The geometrical configuration of the proposed antenna is shown in Fig. 1. This antenna is designed to operate in dual band as 5.8 GHz ISM band (from 5.725 to 5.875 GHz) and 10 GHz X band (from 9.623 to 10.427 GHz). The proposed antenna is implemented on a FR4 substrate with thickness of 1.575 mm, relative permittivity 4.4 and loss tangent of 0.019, while copper patch having a thickness of 0.035 mm is used as the radiating element. MPA was fed using a microstrip feed line which was terminated with a 50Ω SMA connector for signal transmission and antenna simulation.

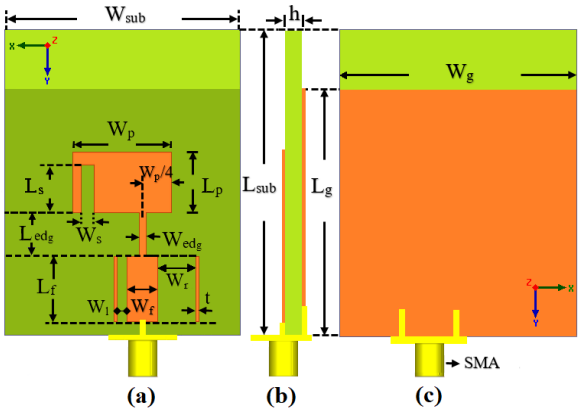

Fig. 1. Configuration of the dual band proposed antenna structure: (a) front view, (b) side view, and (c) back view.

B. Design procedure

In our study, we used the parametric analysis of HFSS at each step and ultimately improved the antenna design parameters. The values given in our paper are in fact the result of many parametric analyzes. Since more details would make the paper too long, we showed only the best results of each parametric analysis in our paper. Also, we give our design methodology as a flowchart shown in Fig. 2.

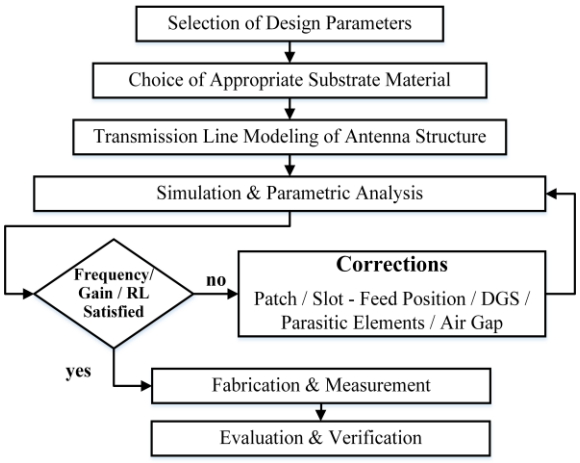

Fig. 2. Flow chart of design methodology.

The antenna development procedure is shown systematically in Fig. 3 within four step.

Initially, even though its loss tangent is relatively high, we preferred the FR4 substrate in our design because of the advantages of being cheap and easy to obtain. The FR4 substrate consists of an epoxy matrix reinforced with woven glass. This composition of epoxy resin and fiber glass varies in thickness and depends on direction [14, 20].

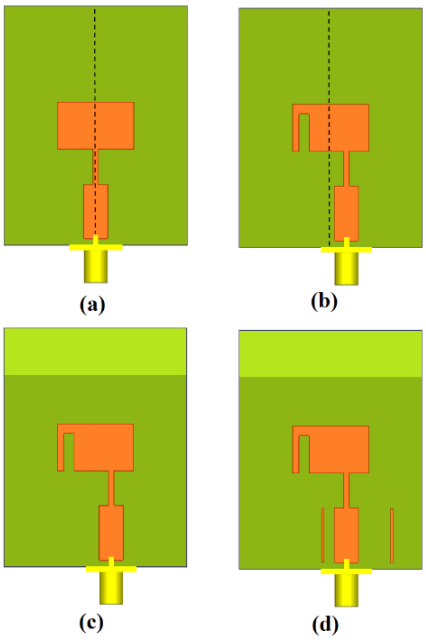

Fig. 3. Antenna design steps: adjusting of (a) initial antenna (Step #1), (b) slot-feed position (Step #2), (c) DGS (Step #3), and (d) parasitic element (Step #4).

In step 1, we obtained the initial dimensions of MPA with the rectangle patch with edge feed by using Transmission Line Model (TLM) for 10 GHz resonance frequency. To operate in the fundamental mode, the length of the patch should be slightly less than $\lambda g/2$, where λg is the wavelength in the dielectric medium and is equal to $\lambda o/\sqrt{\varepsilon_{eff}}$, where λo is the free-space wavelength and ε_{eff} is the effective relative permittivity which can be obtained by the following equation (1) [21]:

$$\varepsilon_{eff} = \frac{\varepsilon_r + 1}{2} + \frac{\varepsilon_r - 1}{2}\left(1 + 12h/W\right)^{-1/2}, \quad (1)$$

where h, W, and ε_r are the thickness of substrate, the width of microstrip patch and relative permittivity, respectively.

The initial antenna was fed from the side by a quarter-wave microstrip line to provide impedance matching. The relationship between resonance length L_{edg} and directed wavelength λg is given equation (2) below [22]:

$$L_{edg} = \lambda_g / 4 = \frac{c}{4 f_r \sqrt{\varepsilon_{eff}}}, \quad (2)$$

where c refers to speed of light and fr is the resonance frequency.

Since the accuracy of the TLM approach is not very good, the results obtained from the simulation with these TLM values do not provide desired characteristics as much. At this point, adjusting of the patch size is necessary for desired characteristics of antenna. This is done by trial and error method and some simulation programs. In our case, parametric analysis tool of HFSS [23] program was used to obtain right size of the patch which is to be used in the next steps shown in Fig. 3 (a). In all the other steps we used the same HFSS tool for optimum performance as well. Some of the different RL curves obtained for different values during these analyzes are shown in each step. By looking at the curves in these figures, the values that yields the best value of RL and gain in the working frequencies were selected.

In step 2, slot opening method was used to obtain dual-band characteristic on a standard rectangular antenna. Firstly, we fixed the feed position at the center and opened a slot on the patch and changed the position of it while observing the return loss variation [24]. As a result, a second frequency (changing from 5 to 7 GHz) with 10 GHz appeared.

Then, the feeding position has been changed for further improvement of the RL [25]. After then, for the intended dual band of 5.8 GHz and 10 GHz frequencies, good results have been obtained with the use and optimization of these two methods together. The resulting antenna is shown in Fig. 3 (b). The return loss change for some different slot lengths and widths values is shown in the Fig. 4.

In step 3, DGS method was used for gain improvement. When we use MPA, the problems which will occurs are surface waves and high loss in the substrate layer. The losses that are due to the surface waves excitation will cause decrease in the antenna gain, efficiency and the bandwidth. When we use DGS on MPA, it reduces the surface waves on the ground plane that reflect from the edge of the ground plane which will influence the current flow and the input impedance of the antenna and therefore changes return loss and increases the gain [26-29].

In this step, in order to increase the gain while maintaining the resonances at the frequencies 5.8 and 10 GHz, the ground surface is optimally removed without overlapping the patch and feed region as shown in Fig. 3 (c). The return loss change for some different ground lengths is shown in the Fig. 5.

In step 4, for further return loss and gain improvement, parasitic element (PE)s were optimally placed parallel to the right and left of the feed line as shown in Fig. 3 (d) [30]. The return loss change for some different locations of parasitic element is shown in the Fig. 6.

The effects of the evolutionary steps on the S_{11} of the antennas designed with the methods explained in steps #1 to #4 used is shown in Fig. 7. Here, since the return loss graphs overlap one another, the return loss change for each step is shown in the Table 1 for a better view of the results. Design stages play an important role on the operating frequency of the antenna. In our design, DGS and parasitic element addition outside the slot opening region as in the Fig. 3, does not change the upper

working band (10 GHz) and the lower working band (5.8 GHz) as seen from Fig. 7.

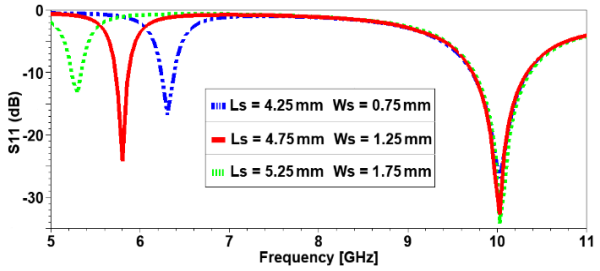

Fig. 4. RL results of the different slot lengths and widths.

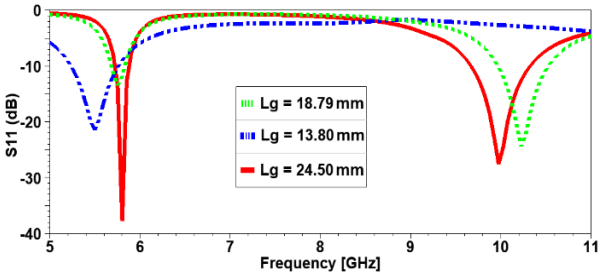

Fig. 5. RL results of different ground (DGS) lengths.

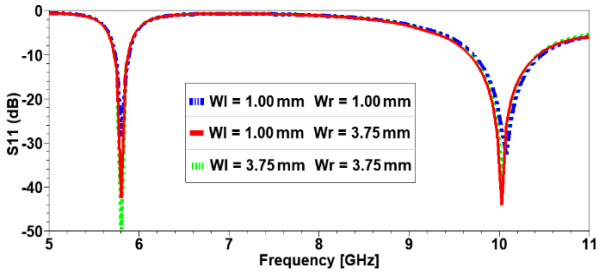

Fig. 6. RL results of different locations of parasitic element.

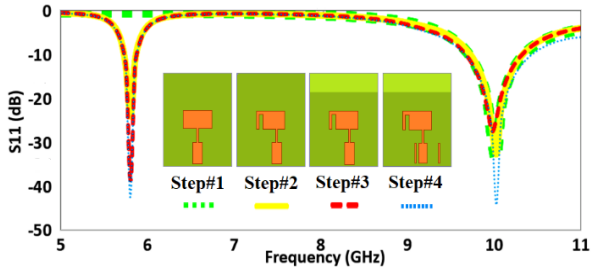

Fig. 7. S_{11} for the steps #1 to #4.

As a final step (Step #5), in order to further increase the gain, under the MPA used in step #4, after an air gap we used a one-sided second layer with the same properties and dimensions as shown in Fig. 8.

The purpose of using a second FR4 layer underneath the antenna is to add an air gap to the structure. Aim of the air gap between the radiating element and the lower ground plane is to reduce high substrate loss of the material used and so increase the gain.

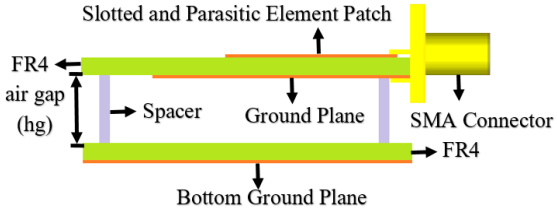

Fig. 8. Step #5: Side view of proposed antenna structure.

Table 1: Comparison of steps in terms of RL

Steps of Design	RL (dB)	
	5.8 GHz	10 GHz
Step #1	-	33.41
Step #2	24.20	32.75
Step #3	38.67	27.57
Step #4	42.52	44.25

For the second layer used, possible situations such as whether the second layer will be over or under MPA, double sided or single sided, top or bottom ground and with or without DGS were analyzed separately. For best results, it was concluded that the ground should be under the second layer without DGS. Next to these, the effect of the air gap on the gain was investigated parametrically with the HFSS.

As a result, optimum value of the air gap thickness, hg was found as 7.5 mm. Since it was observed that insertion of the air gap did not change the return loss much, only the gain versus the air gap thickness has given in Table 2. In this table, the gain describes the peak gain in the boresight direction.

Table 2: Simulated antenna gain versus the air gap thickness

Air Gap, hg (mm)	Gain (dBi)	
	5.8 GHz	10 GHz
3.5	3.56	6,68
5.5	3.72	6,79
7.5	**4.11**	**7,15**
9.5	4.03	6,74

The created air gap reduces both the effective dielectric constant of the radiating plane and the electric field concentration on the lossy epoxy. In the work done, the effective dielectric constant ε_{eff} was reduced by using the air gap to reduce the high insulation loss of the FR4

material [31]. Equation (3) was used to obtain this value which yields ε_{ort} = 1.59 which is smaller than ε_{eff} = 3.57,

$$\varepsilon_{ort} = \frac{\varepsilon_{r1}h + \varepsilon_{r2}h_g}{h + h_g}. \quad (3)$$

Finally, the optimum performance of the antenna was achieved by the parametric studies carried out with the HFSS and the final parameters of the antenna are shown in Table 3.

Table 3: Dimensions of proposed antenna

Parameter	Size (mm)	Parameter	Size (mm)
Lsub	30	*Ledg*	4.3
Wsub	23	*Wedg*	0.7
Lp	6	*Lf*	6.5
Wp	9.6	*Wf*	3
Lg	24.5	*Wr*	3.75
Wg	23	*Wl*	1
Ls	4.75	*t*	0.25
Ws	1.25	*h*	1.575
hg	7.5		

III. RESULTS AND DISCUSSIONS

The main performance parameters of an antenna are RL, surface current distribution, radiation patterns and gain/directivity. For the proposed antenna, these parameters were simulated and obtained using the HFSS. On the other hand, RL measurement were performed using a portable vector network analyzer (ANRITSU MS2028C) covering 10 kHz-20 GHz.

A. Return loss

The return loss (negative of the S_{11}) graphics of the proposed antenna at frequencies of 5.8 GHz and 10 GHz are shown in Fig. 9.

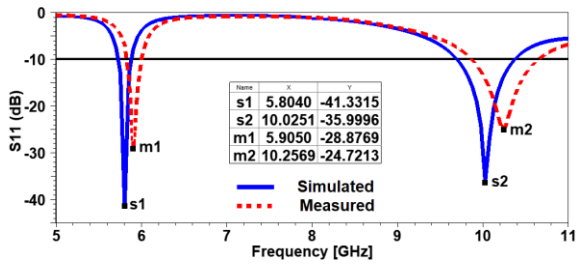

Fig. 9. S_{11} values of the proposed antenna.

The measured result is shifted systematically to higher frequencies. This can be attributed to the incorrectness of the catalog information of the dielectric constant of the epoxy material used or errors in manufacturing and measurement processes.

According to Fig. 9, S_{11} = -10 dB bandwidth of the simulated and measured of the proposed antenna are 160 MHz at 5.8 GHz and 680 MHz at 10 GHz, 176 MHz at 5.8 GHz and 785 MHz at 10 GHz, respectively.

B. Surface current distribution

Looking at the surface current distributions shown in Fig. 10, the current flow at 10 GHz is stronger and more continuous than 5.8 GHz, and is also concentrated at patch edges and quarter wave zones. The figure shows that the slot radiates at 5.8 GHz and the patch at 10 GHz.

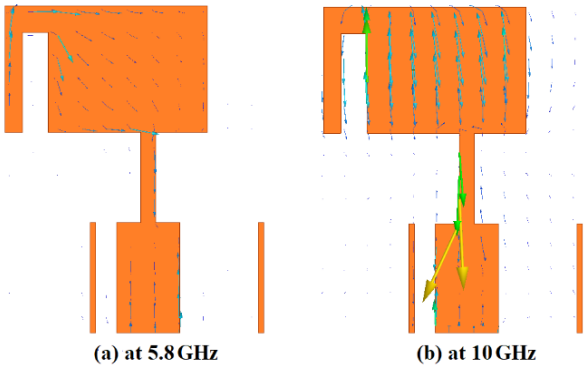

Fig. 10. Surface current distributions on the proposed antenna.

C. Radiation patterns and gain/directivity

The simulated far-field radiation patterns of the proposed antenna at both resonance frequencies are plotted in Fig. 11.

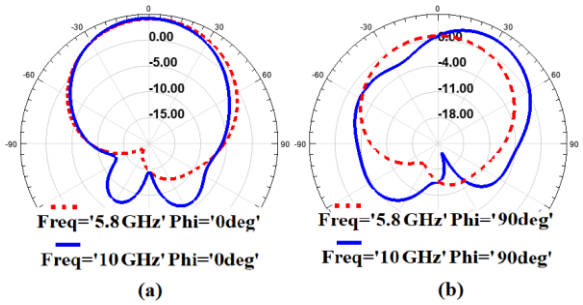

Fig. 11. Simulated far-field radiation patterns: (a) E-plane (x-z) and (b) H-plane (y-z).

The proposed antenna is optimized for the best radiation efficiency, ηre. Radiation efficiency can be defined as the ratio of the output power of the antenna (P_{out}) to the input power (P_{in}) of the antenna and is defined in equation (4) as:

$$\eta_{re} = P_{out} / P_{in}. \quad (4)$$

The directivity and gain of the antenna are related to efficiency as given equation (5) below:

$$G(dB) = \eta_{re} D(dB). \quad (5)$$

The gains of the proposed antenna are 4.11 dBi at 5.8 GHz and 7.15 dBi at 10 GHz, respectively. Figure 12 shows the gain and directivity of the proposed antenna

for frequencies 5.8 GHz and 10 GHz. Here, only a few frequencies have been chosen so that the gain and directivity values are displayed locally.

Table 4: Comparison of design steps in terms of the gain

Steps of Design	Gain (dBi)	
	5.8 GHz	10 GHz
Step#1	–	5.46
Step#2	1.78	5.46
Step#3	2.40	6.26
Step#4	2.28	6.55
Step#5	**4.11**	**7.15**

The proposed antenna is compared with some recently published studies. In terms of several parameters, the comparison is presented in Table 5.

The directivity of the antenna at 5.8 GHz is 6.85 dBi and the gain is 4.11 dBi and the directivity at 10 GHz is 8.65 dBi and the gain is 7.15 dBi. Because FR-4 material is lossy, the efficiency is low. Therefore, the directivity value is much higher than the gain value.

The effects of the evolutionary stages on the gain of the antenna are given in Table 4. In this table, the gain describes the peak gain in the boresight direction.

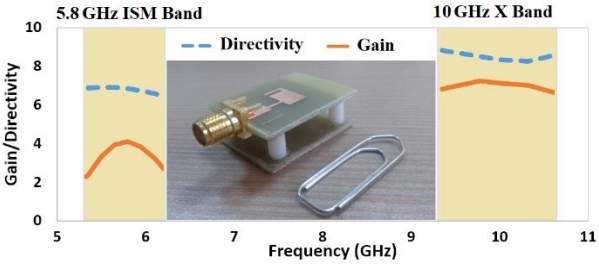

Fig. 12. Gain and directivity for the 5.8 GHz and 10 GHz band.

Table 5: Comparison among other most similar available antennas encountered in the literature

Reference	[13]		[14]			[20]		[32]		[33]		Proposed	
Area (mm^2)	100		1520			1140		484		3600		690	
Height (mm)	1		1.6			1.57		1.6		1		1.57	
Substrate	FR4		FR4			Rogers		FR4		Rogers		FR4	
Resonance Frequencies (GHz)	9.2	11.7	1.5	2.4	4.5	8.2	9.9	3.4	5.5	5.3	6.1	5.8	10
Bandwidth (MHz)	266	450	86	109	284	1028	1030	700	680	230	360	160	680
VSWR	1.04	1.09	1.06	1.24	1.50	1.15	1.16	Not mentioned		Not mentioned		**1.01**	**1.03**
Gain (dB)	4.34	4.59	1.03	1.33	1.84	2.96	4.24	2.04	3.44	7.00	5.00	4.11	**7.15**

IV. CONCLUSION

In this study, it is explained how to increase the gain of a miniaturized dual-band MPA operating at 5.8 GHz and 10 GHz step by step by combining several different methods used in the literature for performance improvement of patch antennas. Design approach consisting of five systematic steps was introduced. Parametric analysis was performed to verify the proposed design and optimize the antenna structure. The results were compared in terms of return loss, standing wave ratio and gain. This antenna can be used in dual-band communication systems for Wi-Fi (5.8 GHz) and Radar (10 GHz) applications. The compatibility of the simulation and measurement results, the compact size of the designed antenna (23 mm × 30 mm), the simple structure and the low cost make the proposed antenna suitable for practical applications.

ACKNOWLEDGMENT

This research was financially supported by the Researching Projects Committee of the University of Dicle (DUBAPK) with project number 14-MF-71. We are grateful to DUBAPK for financial assistance.

REFERENCES

[1] H. Wang and M. Zheng, "An internal triple-band WLAN antenna," *IEEE Antennas and Wireless Propagation Letters*, vol. 10, pp. 569-572, Feb. 2013.

[2] A. Srilakshmi1, N. V. Koteswararao, and D. Srinivasarao, "X band printed microstrip compact antenna with slots in ground plane and patch," *Recent Advances in Intelligent Computational Systems, IEEE*, pp. 851-855, Sept. 2011.

[3] C. U. Ndujiuba and A. O. Oloyede, "Selecting best feeding technique of a rectangular patch antenna for an application," *International Journal of Electromagnetics and Applications*, vol. 5, no. 3, pp. 99-107, May 2015.

[4] L. H. Weng, Y. C. Guo, X. W. Shi, and X. Q. Chen, "An overview on defected ground structure," *Progress in Electromagnetic Research B*, vol. 7,

pp. 173-189, July 2008.

[5] Z. H. Tu, Q. X. Chu, and Q. Y. Zhang, "High-gain slot antenna with parasitic patch and windowed metallic superstrate," *Progress in Electromagnetics Research Letters*, vol. 15, pp. 27-36, Jan. 2010.

[6] R. N. Tiwari, P. Singh, and B. K. Kanaujia, "Dual U-slot loaded patch antenna with a modified L-probe feeding," *Journal Microwaves, Optoelectronics and Electromagnetic Applications (JMOE)*, vol. 16, no. 3, Sept. 2017.

[7] S. Verma and P. Kumar, "Compact arc-shaped antenna with binomial curved conductor-backed plane for multiband wireless applications," *IET Microwaves Antennas and Propagation*, vol. 9, no. 4, pp. 351-359, Mar. 2015.

[8] Y. Li and W. Yu, "A miniaturized triple band monopole antenna for WLAN and WiMAX applications," *International Journal Antennas Propagation*, pp. 1-5, Oct. 2015.

[9] R. Kumar and S. Raghavan, "A compact metamaterial inspired triple band antenna for reconfigurable WLAN/WiMAX applications," *AEU-International Journal of Electronics and Communications*, vol. 69, no. 1, pp 274-280, Jan. 2015.

[10] J. Kaur, R. Khanna, and M. Kartikeyan, "Novel dual-band multistrip monopole antenna with defected ground structure for WLAN/BLUETOOTH/WIMAX applications," *International Journal Microwave Wireless Technologies*, vol. 6, no. 1, pp. 1-8, Sept. 2013.

[11] T. Hirano and J. Takada, "Dual-band printed inverted-F antenna with a nested structure," *Progress in Electromagnetic Research Letter*, vol. 61, pp. 1-6, Jan. 2016.

[12] T. H. Chang and J. F. Kiang, "Compact multi-band H-shaped slot antenna," *IEEE Transactions on Antennas and Propagation*, vol. 61, no. 8, pp. 4345-4349, May 2013.

[13] A. S. Bhadouria and M. Kumar, "Microstrip X-band antenna with improvement in performance using DGS," *Electrical and Electronic Engineering*, vol. 4, no. 2, pp. 31-35, Feb. 2014.

[14] A. Ahmad, F. Syeda, I. Naqvi, Y. Amin, and H. Tenhunen, "Design, fabrication, and measurements of extended L-shaped multiband antenna for wireless applications," *Applied Computational Electromagnetics Society Journal (ACES)*, vol. 33, no. 4, Apr. 2018.

[15] W. Jin, X. Yang, X. Ren, and K. Huang, "A novel two-layer stacked microstrip antenna array using cross snowflake fractal patches," *Progress in Electromagnetics Research C*, vol. 42, pp. 95-108, Jan. 2013.

[16] [Online]. Available: https://www.everythingrf.com/community/ism-frequency-bands.

[17] M. S. Sharawi, M. U. Khan, A. B. Numan, and D. N. Aloi, "A CSRR loaded MIMO antenna system for ISM band operation," *IEEE Transactions on Antennas and Propagation*, vol. 61, no. 8, pp. 4265-4274, Aug. 2013.

[18] M. R. Sobhani, N. Majidi, and Ş. T. Imeci, "Design and implementation of a quad element patch antenna at 5.8 GHz," *Applied Computational Electromagnetics Society Journal (ACES)*, vol. 33, no. 10, Oct. 2018.

[19] B. Datta, A. Das, A. Kundu, S. Chatterjee, M. Mukherjee, and S. K. Chowdhury, "Twice-band irregular rectangular cut-in microstrip patch antenna for microwave communication," *International Conference on Information Communication and Embedded System*, Feb. 2013.

[20] M. T. Islam and M. Samsuzzaman, "Miniaturized dual band multi slotted patch antenna on Poly-tetrafluoroethylene glass microfiber reinforced for C/X band applications," *Hindawi Publishing Corporation the Scientific World Journal*, June 2014.

[21] C. A. Balanis, *Antenna Theory: Analysis and Design*. John Wiley & Sons - Interscience, USA, 2005.

[22] D. M. Pozar and D. H. Schaubert, *Microstrip Antennas, the Analysis and Design of Microstrip Antennas and Arrays*. New York/ABD: IEEE Press, 1995.

[23] Ansoft High Frequency Structure Simulation (HFSS), ver. 15.2, Ansoft Corporation, Pittsburgh, PA, 2015.

[24] A. Elboushi and A. R. Sebak, "High gain hybrid DRA/horn antenna for MMW applications," *IEEE Antennas and Propagation Society International Symposium (APSURSI)*, July 2014.

[25] H. Zhang, U. Zhou, Z. Wu, H. Xin, and R. W. Ziolkowski, "Designs of ultra wideband (UWB) printed elliptical monopole," *Microwave and Optical Technology Letters*, vol. 52, pp. 466-471, Feb. 2010.

[26] A. Desai, T. Upadhyaya, R. Patel, S. Bhatt, and P. Mankodi, "Wideband high gain fractal antenna for wireless applications," *Progress in Electromagnetics Research Letters*, vol. 74, pp. 125-130, Apr. 2018.

[27] A. K. Arya, M. V. Kartikeyan, and A. Patnaik, "Defected ground structure in the perspective of microstrip antenna," *Frequenz*, vol. 64, no. 5-6, pp.79-84, Oct. 2010.

[28] F. Y. Zulkifli, E. T. Rahardjo, and D. Hartanto, "Radiation properties enhancement of triangular patch microstrip antenna array using hexagonal defected ground structure," *Progress in Electromagnetics Research*, no. 5, pp. 101-109, 2008.

[29] D. Marotkar, P. Zade, and V. Kapur, "To study the effect of DGS on antenna parameters,"

International Journal of Industrial Electronics and Electrical Engineering, vol. 3, no. 7, July 2015.

[30] M. R. Zaman, M. T. Islam, N. Misran, and J. S. Mandeep, "Analysis of resonance response performance of C-band antenna using parasitic element," *Hindawi Publishing Corporation the Scientific World Journal*, May 2014.

[31] M. Özenç, M. E. Aydemir, and A. Öncü, "1, 26 GHz rezonans frekansında çalışan çift tabakalı yüksek kazançlı mikroşerit dikdörtgen yama anten tasarımı," *Journal of the Faculty of Engineering and Architecture of Gazi University*, pp. 743, Jan. 2013.

[32] D. K. Naji, "Compact design of dual-band fractal ring antenna for WiMAX and WLAN applications," *International Journal of Electromagnetics and Applications*, vol. 6, vol. 2, pp. 42-50, Sept. 2016.

[33] F. R. Rostami, G. Moradi, and R. S. Shirazi, "Dual-band wide-angle circularly-polarized microstrip antenna by ferrite ring inserted in its cavity domain," *Applied Computational Electromagnetics Society Journal (ACES)*, vol. 32, no. 1, Jan. 2017.

İsa Ataş was born in Diyarbakır, Turkey, in 1975. He received the B.Sc. and M.Sc. degrees Electrical and Electronics Engineering from the Dicle University, Diyarbakır in 2000 and 2011. He is currently a Ph.D. student at Electrical and Electronics Engineering Department of Inonu University. Since 2007, he has been a lecturer at the Diyarbakır Vocational School of Technical Sciences of Dicle University.

His research is focused on linear, planar and miniaturized, high gain, wide band antenna design, microstrip antenna arrays for next generation wireless communication systems. His Ph.D. thesis is related to the design and implementation of high gain microstrip patch antennas.

Teymuraz Abbasov received the B.Sc. and M.Sc. degrees in Electrical Engineering from Moscow Technical University (MAMI), Moscow in 1981 and his Ph.D. degree in Electrical Engineering and Electromagnetic Technology from National Academy Science of Azerbaijan, Baku, Azerbaijan in 1991. His main research interests are mathematical modelling and measurement of electromagnetic field and waves, magnetic separation and filtration processes, numerical modelling of magneto-hydrodynamics and nonlinear electrical circuits, bio-electromagnetic sensors and actuators, MEMS, magnetic fluids theory and applications.

Since 1996, he has been working as a Professor at Inonu University, Malatya, Turkey. His main interests are electromagnetic fields and its applications.

Muhammed Bahaddin Kurt was born in Diyarbakır, Turkey, in 1970. He received the B.Sc. and M.Sc. degrees from the Hacettepe University, Ankara in 1992 and 1996, respectively and Ph.D. degree from the Sakarya University, Sakarya, Turkey in 2002, all in Electrical and Electronics Engineering. Between 1996 and 2005, he worked as a Teaching and Research Assistant in the Department of Electrical and Electronics Engineering at Dicle University, Diyarbakır, Turkey.

Since 2005, he has been working as an Assistant Professor in the same department. His research interests are mainly computational electromagnetics, artificial intelligence, microstrip patch antennas, and non-destructive testing of materials.